

# Signal-to-noise analysis in a counter-pumped fiber Raman amplifier

GEORGH FELINSKYI, MYKHAILO DYRIV\*

Department of Radiophysics, Electronics, and Computer Systems,  
Taras Shevchenko University of Kyiv,  
Academician Glushkov prospect 2, 03-022 Kyiv, Ukraine

\*Corresponding author: dyrivm@ukr.net

The light gain efficiency due to Raman scattering in a distributed fiber Raman amplifier is a subject of our investigation. The detailed analysis of noise properties at one-wave optical signal amplification in a single-mode fiber in the scheme of counter-pumped fiber Raman amplifier is realized in the paper. Experimental results of the amplified spontaneous emission with backward pumping as a base of optical noise evaluation are presented. Raman gain spectrum for a coherent Stokes low-powered signal is calculated and it is compared with the observed spectrum of non-coherent amplified spontaneous emission noise. It is shown that an output optical signal has higher gain than the amplified spontaneous emission and it results in the appreciable growth in the output optical signal-to-noise ratio.

Keywords: amplified spontaneous emission, fiber Raman amplifier, optical signal-to-noise ratio, single-mode fiber, Raman gain.

## 1. Introduction

The creation of light amplifiers based on stimulated Raman scattering (SRS) is regarded to be the most powerful practical achievements [1] in optic telecommunication. At first, practical applications of fiber Raman amplifiers (FRA) with several pumping sources [2] and high-quality amplification of optical signals with a bandwidth close to limiting for silica fibers value about 13 THz have been shown. Such amplifiers are widely applied in spite of the actual interdiction imposed by the theory. Really, the modern theory [3–5] predicts that the noise figure of any optical amplifier should be higher than the minimal quantum limit of 3 dB. It means that the optical signal-to-noise ratio (OSNR) after amplification should be decreased at least by factor of 2.

The generalized quality parameter of any digital communication system is the bit error rate (BER). It directly depends on the OSNR [6] as:

$$\text{BER} = \frac{1}{2} \operatorname{erfc} \left( \sqrt{\frac{10^{\text{OSNR}/10}}{8}} \right) \quad (1)$$

where  $\operatorname{erfc}(x)$  is the complementary error function, OSNR is in dB units. The noise statistics is described by Eq. (1). One makes sure that we can reduce or increase the BER by an order of magnitude changing the OSNR close to 12 dB on +1 dB or -1 dB, respectively. In addition, to increase the signal transfer distance in the communication link, one must not so much try to restore power losses of a signal due to attenuation in a link, but mainly the maintenance of necessary value of OSNR, for example, it should not be smaller than 21.6 dB that corresponds to  $\text{BER} = 10^{-9}$ . Such a bit error rate absolutely satisfies data transmission systems with a bit rate close to 10 Gb/s without additional error correction [1, 6]. It is necessary to put an error correction device into operation or increase the OSNR due to the reduction in a repeater span for larger bit rates. Hence, each optical amplifier, including FRA, theoretically should appreciably increase the BER during the digital information transfer. However, there is an obvious contradiction between the theoretical performances related to optical amplifiers noise and the real practice of their application in the optical fiber systems. In particular, standard optical communication scheme of linear signal regeneration using the sequential application of optical amplifiers becomes theoretically impossible without full signal restoration from the noise, in view of fast error accumulation with the growth in amplifiers amount. Almost twenty years ago it was marked [5] that the physical phenomena which resulted in extraordinarily rare occurrence of errors in digital optical communication systems had not received unequivocal interpretation, and the problem is still open. The same remarks can be related to the noise performance of practical FRA.

Thus, the experimental results of the amplified spontaneous emission (ASE) observation in the single-mode fiber span using the backward pumped distributed FRA are presented in this report. The calculation of the efficiency of signal Raman amplification based on the on-off Raman gain for a low-powered useful signal gives us the opportunity to estimate real OSNR at the fiber output.

## 2. ASE noise measurement and signal gain calculation

### 2.1. Experimental setup

We have observed ASE from the single-mode fiber span in the counter direction to a pump using a commercial FRA unit with a laser diode (LD) pump source at the wavelength 1465 nm. The experimental setup is shown in Fig. 1. The output pump power from LD is directed to the 50 km span of a standard single-mode fiber (SMF). Pumping LD really contains two identical laser crystals but with orthogonal polarizations. Out-

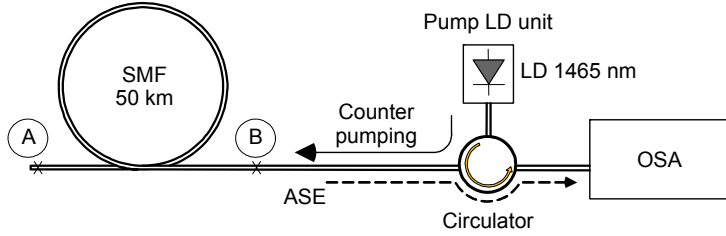


Fig. 1. Experimental setup for measurement of ASE power in SMF with backward pumping.

put LDs powers are summarized using a polarization combiner and it is allowed to remove the polarization dependence of FRA. ASE power from the fiber is registered at the position *B* by an optical spectrum analyzer (OSA). Spectral resolution of OSA was set to 1 nm ( $\sim 4 \text{ cm}^{-1}$ ) for all ASE measurements. Input pump power levels are as follows: 100, 150, 200, 250, and 300 mW. However, the input pump power reduces by over 20% close to the position *B* (end of SMF) because of insertion losses of passive elements of an experimental scheme such as an optical circulator with 0.7 dB losses and connectors with 0.2 dB of insertion losses each. Values of the input pump power before entering the Raman fiber are 77, 116, 155, 194, and 232 mW, respectively.

## 2.2. Simulation model

We applied the system of coupled differential equations [7, 8] for obtaining the output signal power (at 50-km fiber end) with the input power of 1 mW (or 0 dBm). Given theoretical model describes the evolution of optical wave's powers due to propagation along the fiber:

$$\begin{cases} \frac{dP_s(z)}{dz} = g_R(\lambda_p, \lambda_s)P_p^-P_s - \alpha_s P_s \\ \frac{dP_p^-(z)}{dz} = g_R(\lambda_p, \lambda_s)\frac{\lambda_s}{\lambda_p}P_p^-P_s + \alpha_p P_p^- \end{cases} \quad (2)$$

where  $g_R(\lambda_p, \lambda_s)$  is the Raman gain efficiency (RGE) profile in a wavelength domain normalized on an effective fiber area  $A_{\text{eff}}$ ;  $P_s$  and  $P_p$  are signal and backward pump powers, respectively;  $\alpha_s$  and  $\alpha_p$  are attenuation coefficients for signal and pump waves, respectively;  $z$  is the coordinate along the fiber axis. We used the 4-order Runge–Kutta method to solve the system (2). However, as the signal power is small enough for  $P_s \ll \alpha_p/g_R(\lambda_p, \lambda_s)$ , then we can also ignore the pump depletion term in our calculations and solve (2) analytically. Our modeling allows to determine the set of output signal powers using the following parameters:  $g_R(\lambda_p, \lambda_s)$  is taken from [8] and converted to nm units; RGE peak value is equal to  $0.38 \text{ W}^{-1}\text{km}^{-1}$ ,  $\lambda_p = 1465 \text{ nm}$ ,  $\lambda_s = 1520\text{--}1620 \text{ nm}$ ,  $\alpha_p \approx 56 \times 10^{-3} \text{ km}^{-1}$ ,  $\alpha_s(\lambda_s) \approx 51\text{--}49 \times 10^{-3} \text{ km}^{-1}$ , fiber length  $L = 50 \text{ km}$ , fiber length increment  $h = 500 \text{ m}$ ,  $P_{p(z=L)}^- = 100\text{--}300 \text{ mW}$ ,  $P_{s(z=0)} = 1 \text{ mW}$ .

### 3. Results and discussion

The resulting ASE spectra are shown in Fig. 2 for  $\lambda_p = 1465$  nm. The general view of the spectra submitted in Fig. 1 has strongly pronounced features in a qualitative interpretation of the well-known spectrum of spontaneous Raman scattering of light in the silica fibers. It looks like a non-uniform continuum in the Stokes shifts range from 0 up to  $900\text{ cm}^{-1}$ .

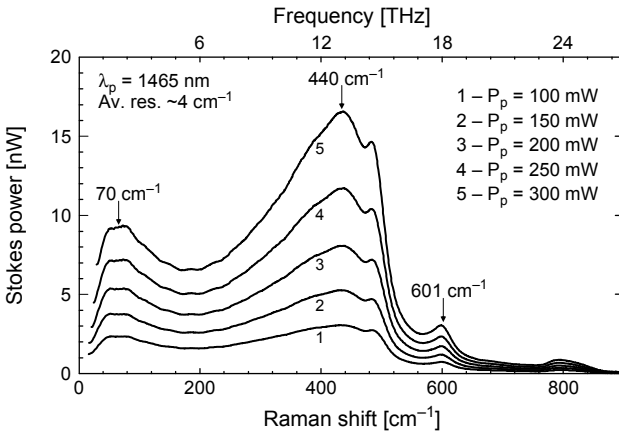


Fig. 2. Absolute Stokes ASE power generated by one LD  $\lambda_p = 1465$  nm in backward pumped FRA with terahertz bandwidth.

The main difference between the spontaneous Raman spectrum and the SRS spectral profile can be extracted as the raised intensity of frequency components with small Stokes shifts approximately up to  $200\text{ cm}^{-1}$ . The measured normalized spectra of output ASE power are shown in Fig. 3 instead of the spontaneous Raman spectrum.

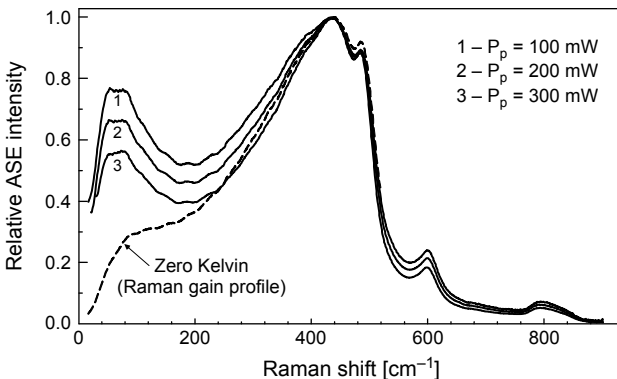


Fig. 3. Normalized Stokes ASE power generated by one LD  $\lambda_p = 1465$  nm in backward pumped FRA. Normalized curves show the trend of ASE distribution to measured Raman gain profile (dashed line) [1] when the pump power is increased.

The graphic comparison between the spontaneous Raman spectrum and the SRS profile (dashed line) is made in Fig. 3 and one can see the similarity between ASE power and spontaneous Raman spectra.

Theoretically, the distinction between the spontaneous and stimulated Raman spectra is directly described by the quantum rate equation [9] for the  $n_s$  Stokes photons created by  $n_p$  pumping photons and  $n_v$  phonons, as:

$$\frac{dn_s}{dz} = C\rho(\hbar\omega_f) \frac{\omega_p\omega_s}{\omega_v} \left[ n_s(n_v + 1)n_p - n_s n_v n_p - n_s n_v + (n_v + 1)n_p \right] \quad (3)$$

where the constant  $C = |\partial\alpha/\partial q|^2 (\pi\hbar^2)/(4V^2Nm\varepsilon_s\varepsilon_p v)$  has been introduced to simplify notation,  $\partial\alpha/\partial q$  is the differential polarizability,  $\mathbf{q}$  is the displacement vector corresponding to  $i$ -th component of the dipole moment,  $\hbar$  is Planck's constant,  $N$  is the number of oscillators in the interaction volume  $V$ ,  $\varepsilon_s$  and  $\varepsilon_p$  are dielectric constants for Stokes and pumping waves, respectively,  $v$  is the phase velocity of Stokes wave,  $\rho(\hbar\omega_f)$  is the density of excited vibration states of molecules in a fiber core,  $\omega_p$ ,  $\omega_s$ , and  $\omega_v$  are the pump, Stokes, and phonon frequencies, respectively.

At the quantum analysis first two terms are often referred to as stimulated emission and stimulated absorption. The last two terms are the spontaneous absorption, and spontaneous emission, respectively.

Since the phonons are assumed to be in equilibrium at the temperature  $T$ , the occupation number  $n_v$  is the thermal equilibrium number,  $n_v = n_B(\omega)$  at that  $n_B(\omega) = [\exp(\hbar\omega/k_B T) - 1]^{-1}$ , where  $k_B$  is Boltzmann's constant. The phonon density factor  $(n_B(\omega) + 1)$  considerably exceeds unit at  $T = 300$  K in the frequency region less than  $200 \text{ cm}^{-1}$  and it infinitely grows when the frequency aspires to zero. A stimulated Raman scattering (SRS) effect forms the Raman gain profile as a zero Kelvin scattering cross-section, which is pointed by a dashed line in Fig. 3.

Alternatively to spontaneous Raman scattering, SRS does not depend on phonon density states and it accordingly does not depend on temperature. It is evident from the Eq. (3) that the difference between first (emission) and second (absorption) terms is equal to  $n_s n_p$ . This fact defines the discrepancy between the observable Raman gain spectrum and the measured spontaneous Raman spectrum and explains the trend of ASE distribution to Raman gain profile when the pump power increases, as one can see in Fig. 3.

Another feature of spontaneous Raman scattering is a linear process by its nature and it does not depend on pump intensity. Because a spontaneous Raman cross-section remains constant for each studied material, the dashed lines in Fig. 4 correspond to spontaneous ASE powers as a function of pump power.

One can see in Fig. 4 the dashed areas which point to the fact that the pure power gain of spontaneous optical noise in a single-mode silica fiber is in the limits bounded by enough small values. Raman quantum efficiency grows no more than  $\sim 80\%$  and it corresponds to the increase in the on-off Raman gain only up to 2.5 dB when the pump powers are increased by factor of 3, *i.e.*, from 100 to 300 mW. It is possible to explain

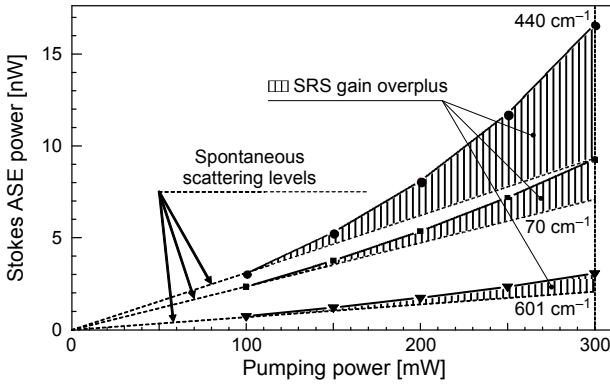


Fig. 4. Stokes ASE power as a function of pump power for several peaks in experimental spectra in Fig. 2 (solid dots). Dashed areas show that the Raman gain values are only decimal parts in comparison with spontaneous scattering levels.

such situation from the physical point of view as follows. Rather weak ASE generation in the studied pump power range results from the lack of coherence of the Stokes photons arising from non-elastic scattering of pump photons on huge amount of molecular phonon vibrations with different frequencies. Therefore Stokes radiation in addition to its random phase distribution appears as distributed in a very wide frequency diapason. Both these circumstances obstruct automatic establishing of the phase matching conditions necessary for coherent accumulation of Stokes radiation which would give the Raman gain. In other words, Raman interaction in the core of the silica based optical fiber results in the “spreading” of pump power along the wide spectrum of Stokes frequencies.

As the creation probability of the in-phase Stokes photons with equal frequencies inversely depends on Raman radiation bandwidth, it means that the available pump power is insufficient for effective Raman noise generation. As a result, spectral power distribution of ASE observed by us looks more like the spontaneous Raman scattering, instead of SRS.

It should be noted that presented results are received without optical signals in a studied single-mode fiber piece. At the presence of a signal, the coherent signal power with spectral density considerably higher than the Stokes noise density starts the concurrence for possession of the pump power during the SRS process. Therefore, the ASE gain coefficients measured by us in the single-mode silica fiber have the greatest possible values and the noise power of real FRA cannot exceed the absolute values resulted from Fig. 2.

The contribution of Raman scattering to signal power is negligible in the case of signal amplification with counter pumping, consequently the output signal power stays the same and reaches the value almost from 61 to 72  $\mu\text{W}$  within the wavelength range 1520–1620 nm or in the diapason of C+L telecommunication window when pumping

is off. It means that the ratio of signal (ASE) power from “mixture” of spontaneous-SRS to signal (ASE) power just from spontaneous scattering is a parameter of the Raman on–off gain. At the presence of pumping, the output signal power becomes almost twice as good owing to SRS interaction between the pump and signal waves when the input backward pump power equals 100 mW. We made our calculation for the investigated signal wavelength 1566 nm, because it enters into the range of least optical losses for a given type of a fiber. We used experimental results for ASE also at the wavelength 1566 nm. All wavelength spectra of the on–off Raman gain within total telecom C+L-window for a signal and ASE noise are shown in Fig. 5.

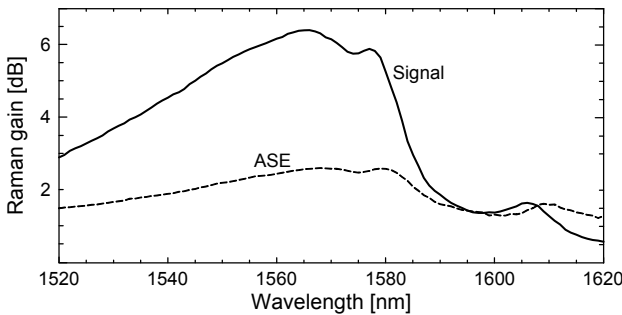


Fig. 5. Calculated on–off Raman gain spectra of coherent Stokes signal (solid line) and non-coherent Stokes noise (dashed line) at pumping power of 300 mW.

So, the on–off Raman gain for a signal 1566 nm is 6.4 dB, whereas ASE gain does not exceed 2.54 dB at the input pump power 300 mW. These data values are maximal in the range of 1520–1620 nm. Higher efficiency of signal amplification in comparison with a pure ASE gain is also proved by significant OSNR. For example, OSNR at the fiber output is equal to 42.8 dB with the input pump power 300 mW. The real output OSNR must be higher than the calculated one 42.8 dB, because ASE noise becomes maximal at signal absence and reduces at signal presence in an optical fiber. Moreover, ASE noise practically has no effect on signal power magnitude.

It is evident that the profile of the on–off Raman gain spectrum repeats the shape of the Raman gain efficiency coefficient  $g_R(\lambda_p, \lambda_s)$  as much as the gain exponentially depends on the input pump power, and on the coefficient  $g_R(\lambda_p, \lambda_s)$  for the case of a single signal and pump waves [7]. The Raman gain spectrum of ASE is smoother. It is caused by the equivalence of spontaneous Raman scattering and SRS processes for the influence on the output ASE power. In the case of signal amplification, the influence of SRS on output signal power is several times greater than the effect of spontaneous Raman scattering. However, the Raman gain of ASE predominates in the signal Raman gain at the wavelength above value of 1610 nm. It is explained by an increase in signal attenuation coefficient and an increase in the Raman effect threshold, respectively [10]: optical losses substantially exceed signal Raman amplification at pumping

of 300 mW. In particular, the output power of a signal at the wavelength 1620 nm with input backward pumping of 300 mW is equal to the signal output power at 1566 nm when the pumping is off and smaller by factor of 10 than the input signal power.

## 4. Summary

Significant difference between the coherent Raman amplification and ASE gain has been found in our work. Our experimental data confirm that the efficiency of Raman amplification of ASE does not exceed 80% and calculations show that the on-off Raman gain is no more than 2.6 dB for ASE at 1566 nm whereas it is  $\approx 6.4$  dB for a useful signal with the input power 1 mW. Signal Raman amplification is determined using a standard numerical technique based on the optical wave's propagation equations. The signal Raman gain is predominated by the ASE one almost everywhere inside C+L telecommunication window in FRA.

Physical reasons of low ASE efficiency and high OSNR performance are discussed. Raman effect in the core of the optical fiber leads to broadening of pump power due to a wide range of Stokes frequencies. Since the probability of in-phase Stokes photons of the same frequency is inversely dependent on the bandwidth of Raman radiation, the available pump power is insufficient for effective amplification of Stokes noise. As a result, we observe spectral distribution of ASE power, which looks like a rather spontaneous Raman scattering but not SRS. It is shown that the backward-pumped 50-km single-mode fiber Raman amplifier has a high OSNR performance (above 42 dB) that leads to a reduction in a real noise figure distinctly below the quantum limit.

*Acknowledgements* – We would like to thank Dr. P. Korotkov for fruitful discussions on the experiment and modeling and his assistance in writing this paper.

## References

- [1] ISLAM M.N., *Raman amplifiers for telecommunications*, IEEE Journal of Selected Topics in Quantum Electronics **8**(3), 2002, pp. 548–559.
- [2] KIDORF H., ROTTWITT K., NISSOV M., MA M., RABARIJAONA E., *Pump interactions in 100 nm bandwidth Raman amplifier*, IEEE Photonics Technology Letters **11**(5), 1999, pp. 530–532.
- [3] YAMAMOTO Y., INOUE K., *Noise in amplifiers*, Journal of Lightwave Technology **21**(11), 2003, pp. 2895–2915.
- [4] HAUS H.A., *Noise figure definition valid from RF to optical frequencies*, IEEE Journal of Selected Topics in Quantum Electronics **6**(2), 2000, pp. 240–247.
- [5] HENRY C.H., KAZARINOV R.F., *Quantum noise in photonics*, Reviews of Modern Physics **68**(3), 1996, pp. 801–853.
- [6] AGRAWAL G.P., *Fiber-Optic Communication Systems*, 3th Ed., John Wiley & Sons, New York, 2002.
- [7] BROMAGE J., *Raman amplification for fiber communications systems*, Journal of Lightwave Technology **22**(1), 2004, pp. 79–93.
- [8] NAMIKI S., EMORI Y., *Ultrabroad-band Raman amplifiers pumped and gain-equalized by wavelength-division-multiplexed high-power laser diodes*, IEEE Journal of Selected Topics in Quantum Electronics **7**(1), 2001, pp. 3–16.



- [9] ROTTWITT K., BROMAGE J., STENTZ A.J., LUFENG LENG, LINES M., SMITH H., *Scaling of the Raman gain coefficient: Applications to germanosilicate fibers*, *Journal of Lightwave Technology* **21**(7), 2003, pp. 1652–1662.
- [10] DYRIV M.Y., FELINSKYI G.S., KOROTKOV P.A., *Fiber attenuation irregularities and simulation of Raman amplification band*, 12th International Conference on Laser and Fiber-Optical Networks Modeling (LFNM), September 11–13, 2013, Sudak, Crimea, Ukraine, pp. 44–46.

*Received April 29, 2014  
in revised form July 10, 2014*